

Supporting Information

Genetically Expanded Reactive-Oxygen-Tolerant Alcohol Dehydrogenase II

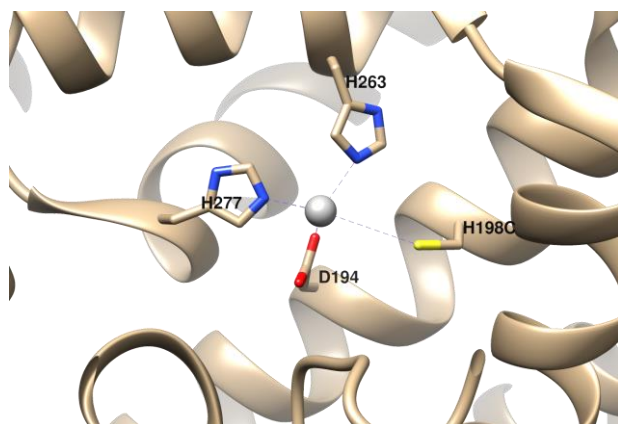
Ashok Kumar Bhagat¹, Hadar Buim¹, Guy Shmul², Lital Alfonta^{*1}

¹*Departments of Life Sciences, Chemistry and Ilse Katz Institute for Nanoscale Science and Technology, Ben-Gurion University of the Negev, Beer-Sheva 84105, Israel.* ²*Department of Chemical Research Support, The Weizmann Institute of Science, Rehovot 7610001, Israel*

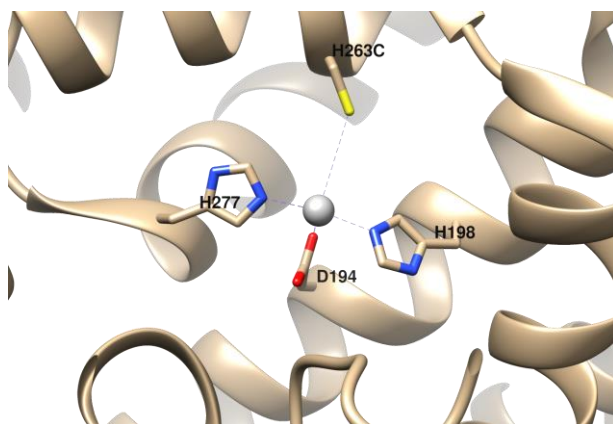
*Corresponding author: Lital Alfonta; alfontal@bgu.ac.il

Table of contents:

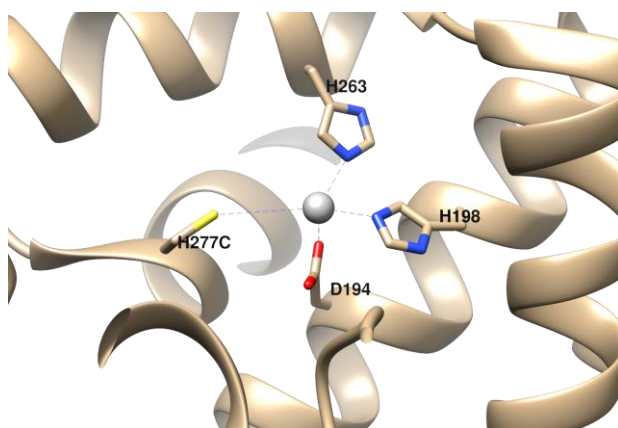
Figure. S1	Mutants created by site-directed mutagenesis	S1
Figure. S2	ITC results for FeCl₃ titration to the WT and mutant ADHII	S2
Figure. S3	Catalytic activity of WTADHII in the presence of zinc (<i>in vitro</i>)	S3
Figure. S4	Ethanol production by ADHIIDOPA and ADHII in vivo in <i>E. coli</i>	S4
Figure. S5	Lineweaver-Burk plots of catalytic activity of ADHIIDOPA	S5
Figure. S6	CVs of rGO/MB/ADHII/GCE	S6
Figure. S7	CVs of electrocatalytic reduction of acetaldehyde in the presence of H₂O₂	S7
Figure. S8	Catalytic activity of H277F and H277Y ADHII	S7



H198C



H263C



H277C

Figure S1. Models of active-site mutants of ADHII (constructed using UCSF Chimera); Mutated amino acids in the active site of ADHII and predicted binding mode of the active-site, displaying Zn (II), center sphere, silver. Mutants are: H198C, H263C and H277C. Cysteine (C) is shown in yellow.

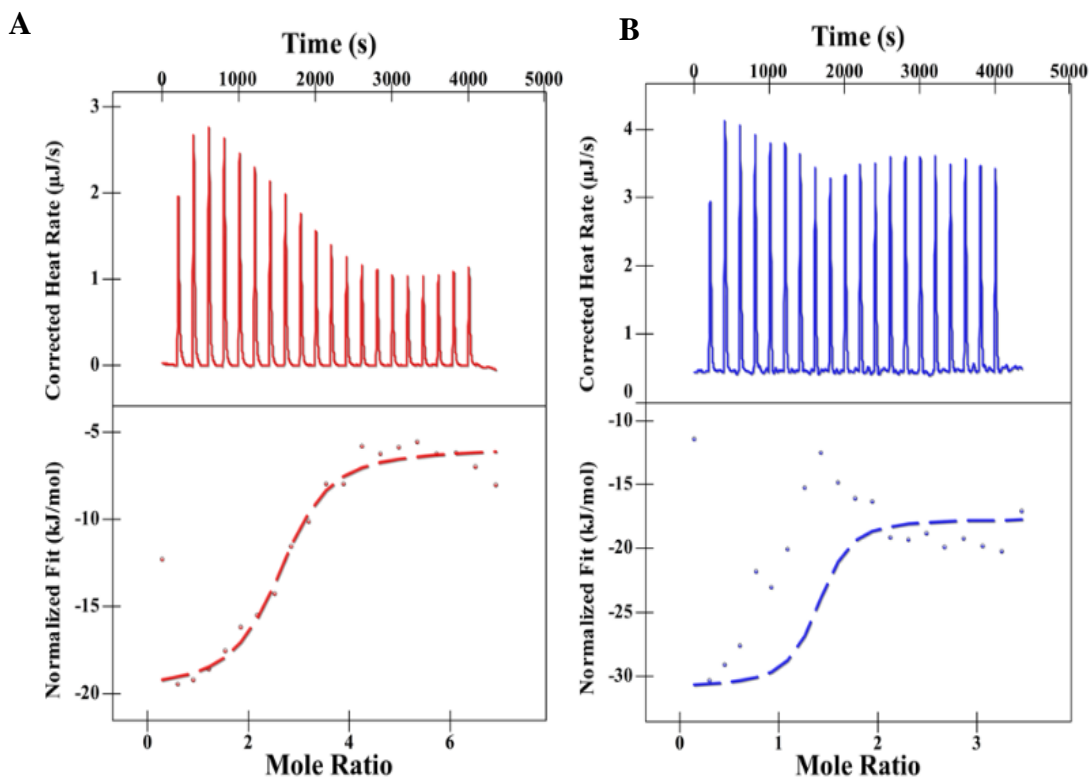


Figure S2. ITC results of FeCl_3 titration to the WT and mutant ADHII. (A) WT ADHII (red) (B) DOPAADHII (blue). It could be seen from the DOPAADHII blue curve that there is no fit, indicating no binding of iron ions upon its titration to the enzyme solution.

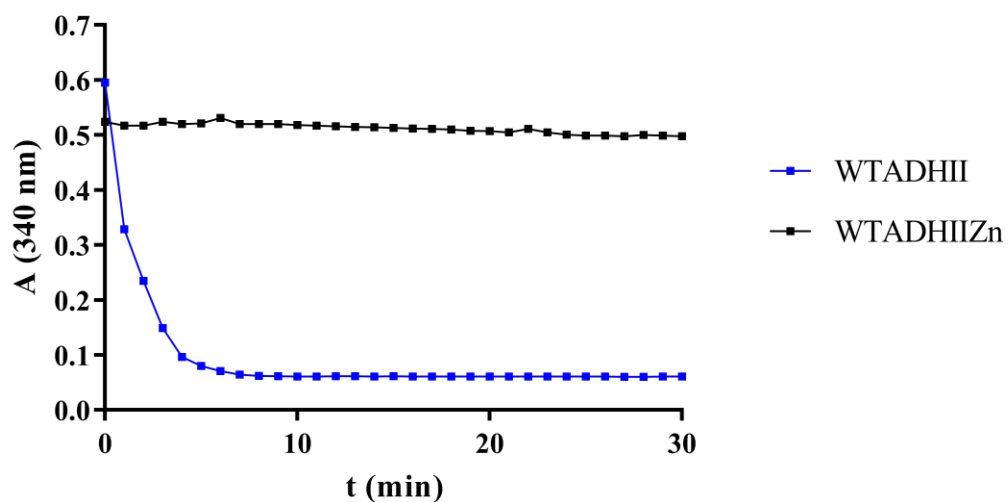


Figure S3. Catalytic activity of WTADHII in the presence of Zn^{2+} (*in vitro*).

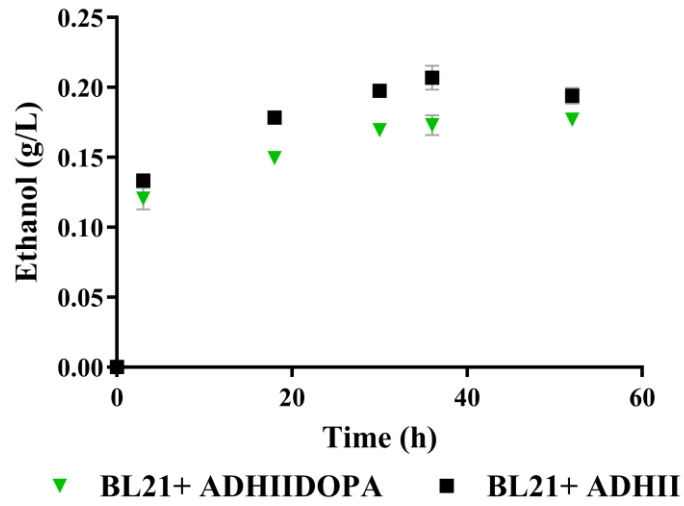


Figure S4. Ethanol production by ADHIIDOPA in the presence of Zn^{2+} in vivo in *E. coli*. Zn^{2+} was not added to the cells expressing WT ADHII (as it was shown to be inactivating). Hence, it could be seen that in vivo, mutant and WT cumulative ethanol production activities are comparable when exogenous zinc is added to the growth media.

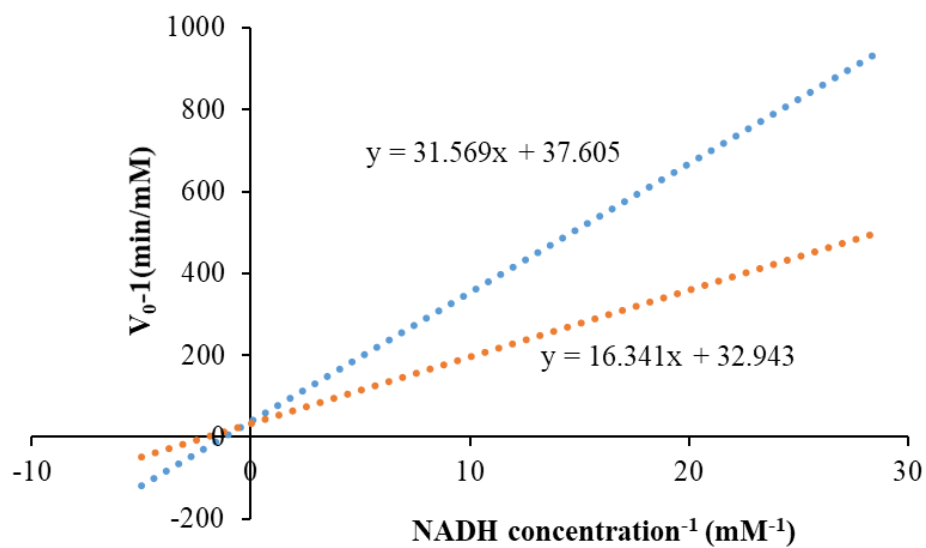


Figure S5. Lineweaver-Burk plots of ADHII catalytic activity of mutant ADHIIDOPA in the presence (orange curve) and absence (blue curve) of hydrogen peroxide. The turnover rates of the mutant were extracted from these plots and are shown in table 3 of the manuscript.

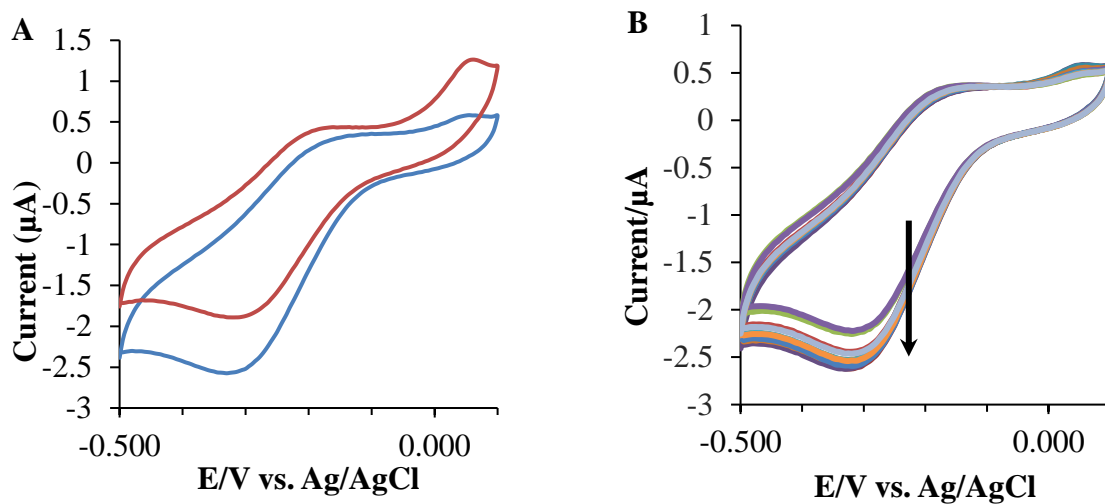


Figure S6. (A) Representative cyclic voltammograms (CVs) of reduced graphene oxide/ methylene blue/ WTADHII/ Galssy Carbon Electrode : rGO/MB/WTADHII/GCE for acetaldehyde reduction in the presence (blue) and absence (red) of acetaldehyde (13 mM). Scan rate is 5 mV/s. Potential step: 0.005V (vs.Ag/AgCl), 100 μM MB was used as a redox mediator and 2 mM NADH was used as a cofactor; reference electrode: Ag/AgCl.; (B) CVs for successive additions of acetaldehyde from 1-10 mM, acetaldehyde reduction potential is measured at (-) 0.320 V vs Ag/AgCl.

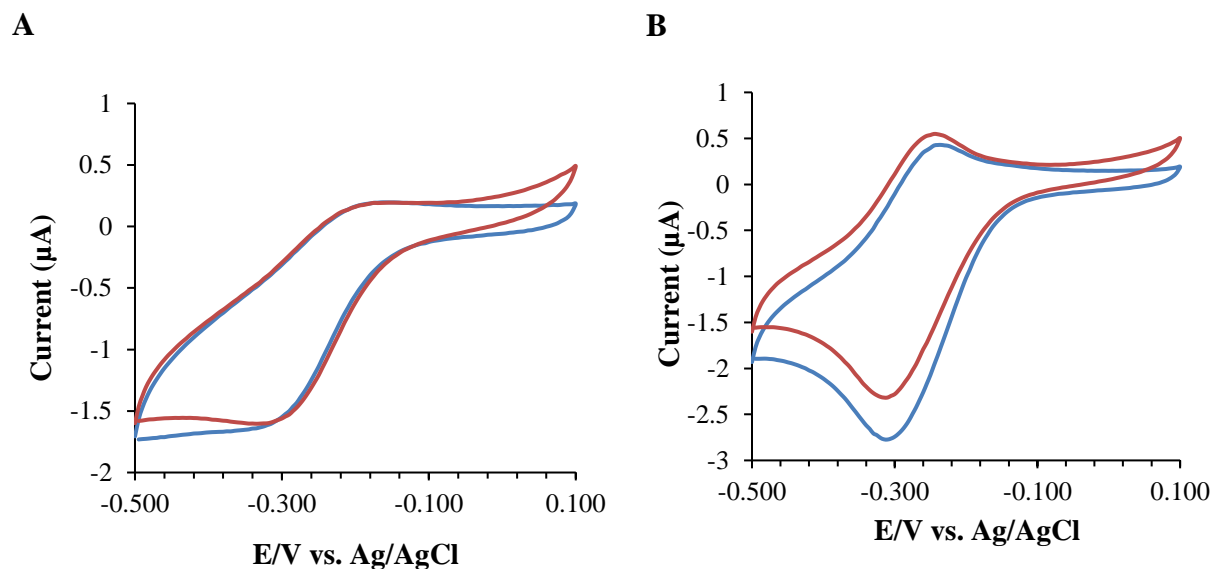


Figure S7. CVs of H_2O_2 treated WT and mutant ADHII modified electrode with (blue) and without (red) 10 mM acetaldehyde. (A) rGO/MB/WTADHII/GCE; (B) rGO/MB/ADHIIIDOPA/GCE. CVs were performed at a scan rate of 5 mV/s in PB (pH 7.0).

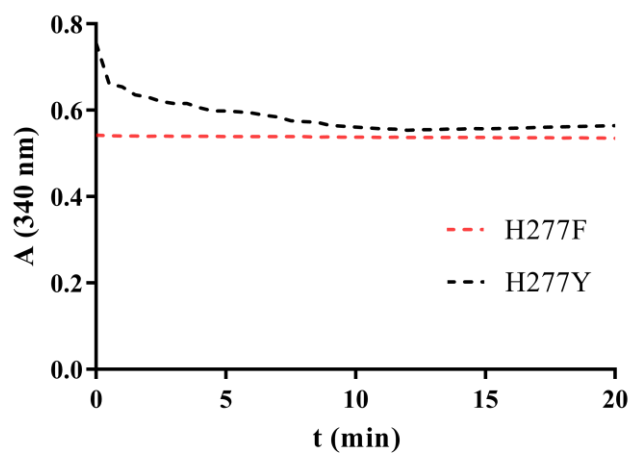


Figure S8. Catalytic activity of mutants H277F, and H277Y ADHII (0.25 μM)